Virtual Surveyor based Segmentation and Hierarchical Decomposition of 3D Image Segments derived from LiDAR Data

Ahsan Habib[1], Venkat Devarajan[1,] and Collin McCormick[2]
The University of Texas at Arlington, Texas, USA
Natural Resources Conservation Service (NRCS), Fort Worth, Texas, USA

***Abstract* - Traditional nonparametric segmentation method relies on segmentations at different scales to produce a hierarchy of semantically significant objects. Properly tuned scale parameters are, therefore, imperative in these methods for successful subsequent classification. Recently, some progress has been made in the development of methods for automatic segmentation scale parameter tuning. However, researchers found that it is very difficult to automatically refine the tuning with respect to each object class present in the scene. Therefore, the method fails to deliver correctly many of the new segment features. In this paper, a new 3d segmentation method is described in detail, which segments objects based on their distinct geometric concavity/convexity. This is achieved by strategically mapping the sloping surface which connects the object to its background. Further analysis produces hierarchical decomposition of objects to its sub-objects at a single scale level. Extensive qualitative results are presented to demonstrate the efficacy of this segmentation approach.**

I. Introduction

The availability of massive amount of high-quality LiDAR data gives us an unprecedented opportunity to extract useful and accurate information for a wide variety of applications. For instance, hierarchical object representation offers new possibilities to gain insight into the content of a given digital image. Unlike object detection, which detects objects of a certain class (such as buildings, or trees) in a given digital image, object representation aims to address the whole scene [1]. Here, the entire topographic map is first segmented into its constituent image-objects that closely represent real-world objects. Object-based image analysis (OBIA) framework has gained traction recently in remote sensing and geographic information science for doing image analysis via object representation. Unlike traditional pixel-based classification approaches, which are based exclusively on the attributes associated with each pixel, OBIA takes advantage of new geographic information reveal by the object representation of the image [2]. OBIA involves two steps: image segmentation and object classification. Firstly, a segmentation algorithm is applied to partition the image into a relatively homogeneous group of pixels referred to as object candidates. This results, in addition to spectral values, in a plethora of new information such as aggregated spectral pixel values, morphology, texture, context as well as topology. These features can be exploited in the subsequent identification of the object candidates by a classifier.

Automatic separation of the topographic surface and its overlying 3D objects using LiDAR data is a challenging problem, especially in complex environment and rough terrain. Arefi in his 2005 paper [3], pointed out this automated segmentation as one of the major and unsolved problems for interpreting LiDAR data. In present, after more than a decade later, generic solution to this problem has not yet been discovered, as pointed out in a recent survey paper [4]. Nevertheless, extensive research has been conducted in this direction. Golovinskiy et al. [5] present a min-cut based method for extracting small urban objects from a combined Airborne and Terrestrial LiDAR point cloud data. Yao et al. [6] proposed a 3d segmentation method combining non-parametric clustering with spectral graph clustering to extract flyovers and vehicles in urban areas from raw airborne LiDAR data.

LiDAR-based object detection and extraction work mainly concentrate on man-made features and few very distinguishable natural features such as trees. Natural objects, commonly referred as landforms [7] is way more difficult to detect than that of a man-made object [1]. Over the last decade, a new branch has emerged from OBIA, termed as Geographic Object-based Image Analysis (GeOBIA) to tackle this problem. The Multi-resolution segmentation (MRS) algorithm [8] has recently garnered a lot of attention within the GeOBIA domain for the delineation of landforms. Dragut, et al [9] employ MRS to segment elementary forms from Digital Elevation Maps (DEMs) based on the homogeneity of elevation derivatives such as gradient, aspect, profile curvature and plan curvature. However, landforms are composed of

multiple such landform elements [10]. Wu et. al. [11] used MRS in LiDAR nDSM image, equipped with different scale parameter, elevation criterion, and shape criterion to extract different urban land cover types.

In the MRS algorithm, choosing the right scale parameter is crucial, since it has a direct effect on the classification accuracy [12]. It is challenging to obtain scale parameter automatically for every object class present in the scene [13]. This leads to over-segmentation and under-segmentation. Moreover, hierarchical relations among objects derived at different scales are difficult to establish. For example, the boundaries shared between objects and sub-objects in the real-world scenario may not coincide in their corresponding resultant segments due to the imprecise selection of the scale parameters.

The current object extraction method, therefore, cannot fully exploit the leverage the object based approach brings to the classification process. We attempt to overcome these limitations in our proposed methodology.

In our approach, the object extraction method is inspired by how a human surveyor, placed on the target object, would plan her path so that she gradually covers and maps the slope of the entire object without any external help. In essence, this method is presented with the same set of data as the human surveyor and it adaptively analyses the data much like the human surveyor would. Hence, the name Virtual Surveyor. The result obtained via virtual surveyor based segmentation method is then fed into the hierarchical decomposition sub-algorithm, which decomposes the image objects to its constituent (if any) sub-objects, while operating at a single scale. The hierarchical relationship between the parent object and its sub-objects is also identified in the process. The entire segmentation process ensures that objects and sub-objects (natural or man-made) of all sizes and shapes and at all levels of the hierarchy can be extracted without requiring to traverse through multiple scales.

II. Methodology

The input to the virtual surveyor based object extraction algorithm is the mesh representation of the terrain. The algorithm has two main components: (1) a seed growing segmentation sub-algorithm that segments the target object from its topographic background, (2) a hierarchical decomposition sub-algorithm, where the extracted image object is analyzed and their sub-objects are extracted.

A. Virtual surveyor based segmentation

The virtual surveyor based segmentation is built upon the two following assumptions:

(1) An object introduces a distinct geometric concavity or convexity on its topographic background. That is, an object can be categorized into either of (or a mixture of) two fundamental 3D geometric structures: convex-like structure and concave-like structure. For example, hills, trees, buildings, drumlins, etc. can be categorized into the convex-like structure category, whereas watershed, swimming pool, gully, crater etc. fall into the concave-like structure.

(2) An object, no matter how complex, is connected to its topographic background via a single enclosed sloping surface. We call this sloping surface as ‘foothill_slope’. Figure 1 shows a stylistically illustration of the foothill_slope of a multistory building and a hill. In the case of a convex structure, normal to all points on the foothill_slope point outward, whereas for the concave object, they point inward. Mapping the foothill_slope will enable partitioning of the object from its background. Any loop (path) which encircle the object and contained within the foothill_slope obey the following properties:

The normal to any point of the loop points inward (or outward) all through in case of concave (or convex) structure.

These loops are referred as ‘path_loops’. For each point on the foothill_slope, there exists one such path_loop to which it belongs to as a constituent.

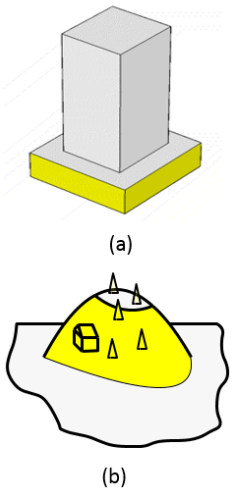

Figure 1 The enclosed sloping surface colored yellow is the foothill_slope of (a) a building, (b) a hill

The foothill_slope mapping process relies on the condition foothill_slope offers (as mentioned in assumption 2) i.e., normal to each point of the enclosed foothill_slope surface is either pointing inward (in the case of convex structure) or outward (concave structure).

As explained in details in our paper [14], if a surveyor, placed on the object, follows a special vector (referred to as surveyor guidance vector), which is estimated in situ, then this would guarantee that at each point of her route, the normal points to the right of the direction of the surveyor. If the path gradually forms a loop, this indicates the formation of a path_loop. The surveyor guidance vector ($\vec{r}$) at a point is calculated using the cross-product of the vertical vector ($\hat{z}$) and the normal ($\hat{n}$) at that point. An example is shown in figure 2.

$$\vec{r} = \hat{z} \times \hat{n} = |\hat{z}||\hat{n}|sin\theta\hat{r} = sin\theta\hat{r} \qquad (i)$$

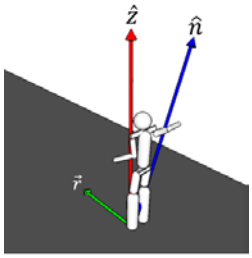

Figure 2 Surveyor standing on a slope

The mathematical formulation of the foothill_slope condition adapted for the mesh representation of the terrain surface is given below:

With referring to figure 3, cell A is the current location of the virtual surveyor and cell B is one of its neighbors. Here, 'first_dot_prod' is the dot product between $\hat{r}_A$ and $\vec{v}_{AB}$ and 'second_dot_prod' is the dot product between $\hat{r}_B$ and $\vec{v}_{AB}$

$$(first\ dot\ prod) \times (second\ dot\ prod) \geq 0\ (iii)$$

We call this condition as 'foothill_slope_criteria'. Neighbors that satisfy the foothill_slope_criteria guarantee the direction of normal ($\hat{n}$) falls on the right all through the path vector.

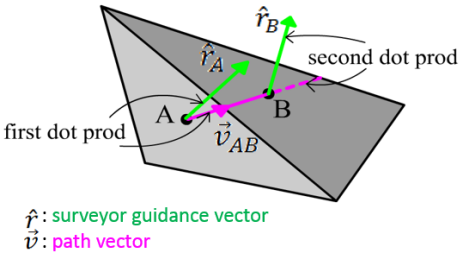

Figure 3 Selecting neighbor

The seed growing segmentation method includes those neighbors into the growing region. This guarantees the mapping of the entire foothill_slope of the target object.

While mapping the foothill_slope of the object, the foothill_slope of the sub-objects (if any) are also accepted into the growing region. An example is shown in Figure 1(b). Here, the hill is the parent object and the house and the trees are its sub-objects. The foothill_slope of the house and the trees has at least some part to which virtual surveyor can move onto from the foothill_slope of the hill without violating the foothill_slope condition. Once the virtual surveyor moved onto the foothill_slope of the sub-objects, the surveyor maps the foothill_slope of the sub-objects. So, in the next step, the composite object is decomposed to reveal its sub-objects.

B. Virtual surveyor based hierarchical decomposition

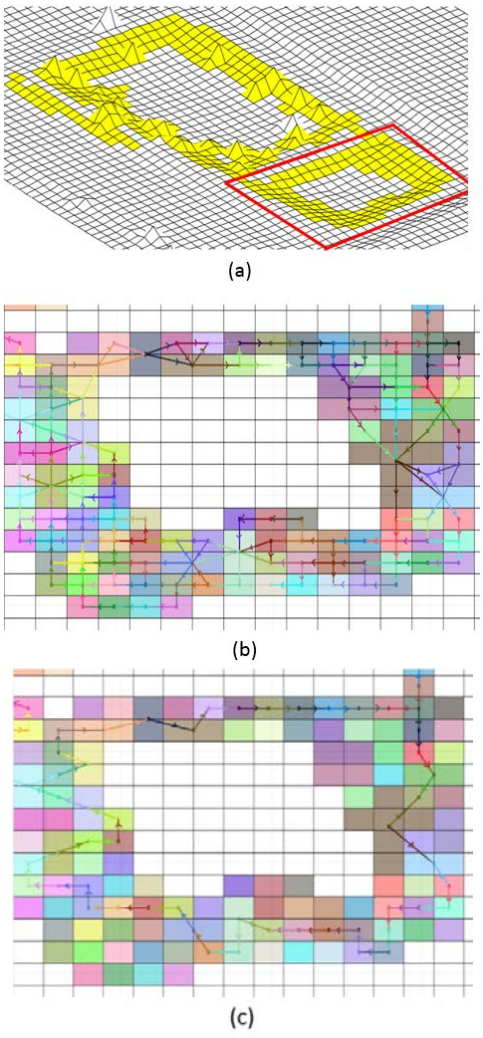

Figure 4 (a) Segmentation result of the pair of adjacent artificial pond, (b) complete_flow_graph of one of the pair (bounded by the red box), and (c) derived representative_path_loop

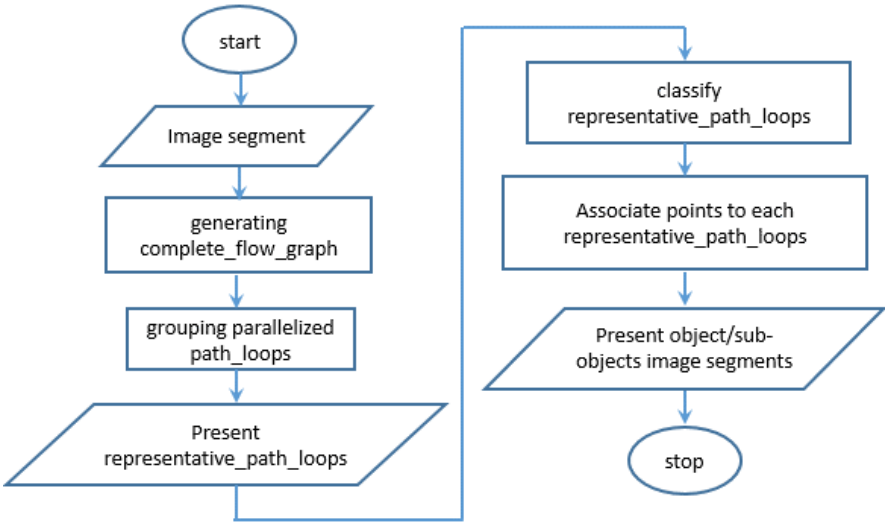

Figure 5 Algorithmic flow-chart of the hierarchical decomposition sub-algorithm

The first and foremost goal of this sub-algorithm is to verify whether the segmentation result is indeed an image representation of a real-world object. The secondary goal is to expose its sub-objects. The sub-object can be an element of the object or can be an independent object. The identity of the sub-object and its relationship to the parent object will be clarified in the later identification step. The flow chart for the hierarchical decomposition is shown in figure **5**. In the following, individual parts of the flowchart are explained in details.

We start by constructing a graph, where each node represents the centroid of a cell in the mesh representation and each connections obeys the foothill_slope_criteria. The graph would capture all the possible path_loops exist in the image segment. That includes the path_loops belong to its sub-objects. This graph is referred as 'complete_flow_graph'. A real-world example of the complete_flow_graph of one of the artificial pond is shown in figure 4(b).

The complete_flow_graph contains two types of loop, circular loops, and parallel loops. A stylistic simulated example of each kind is shown in figure 6. A sub-algorithm is employed that finds all the loops of the directed graph.

Next, we attempt to simplify the graph. Circular loops of small size that satisfy the foothill_slope_criteria are retained and the rest of the circular loops are eliminated. Parallel loops are also strategically merged. So, what remains are a single path_loop for the parent object and for each of its sub-objects. These special path_loops are grouped from their corresponding set of parallelized path_loops, so they are called 'representative_path_loops'. Figure 4(c) illustrate the representative_path_loops derived from the complete_flow_graph as shown in figure 4(b). In the end result, each of these special loops correspond to the sub-objects, are connected to the representative_path_loop of the parent object. This association reveals the hierarchical relationship of the object and its sub-objects.

Each point of a sub-objects, that is not a member of the corresponding representative_path_loop, is connected to that loop by a chain of connections. Based on these connections, these points are associated with their representative_path_loops. Thereby segmentation of its sub-objects can be achieved. Thereby, the decomposition is conducted without traversing through multiple levels of the scale.

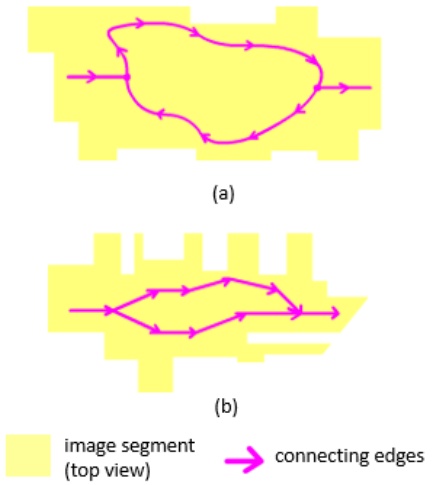

Figure 6 Stylistic Simulated example of (a) circular loop (b) parallel loop

III Result

In this section, we would discuss some of the qualitative results obtained so far.

Figure **7** shows an oblique view of the segmented result of landforms. This is a very interesting case, where the foothill_slope of two neighboring landform, a hill and a watershed, share some part.

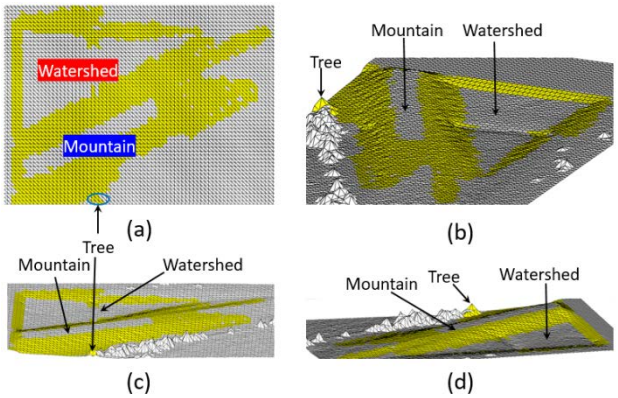

Figure 7 Illustration displaying segmentation result for a hill shaped and watershed shaped landform at (a) top view, and at (b, c, d) different angle views

For this reason, both are segmented from their surrounding using a single seed. In the next step of the hierarchical segmentation algorithm, both will be individually identified.

Figure **8** show the segmentation result of a complex building. It is evident from the figure that all the walls of the building have been successfully mapped.

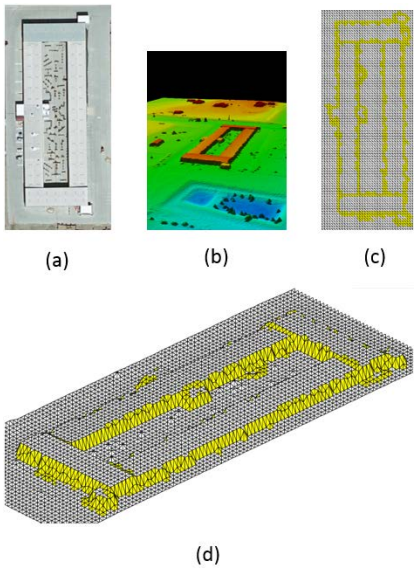

Figure 8 Illustration displaying (a) orthoimage of a complex building, (b) point cloud model of the building, segmentation results at (c) top view, and (d) Oblique view

Figure **9** shows the decomposition result of the complex landforms segment (figure **7**). Their neighborhood and hierarchical relationship are also specified in the figure.

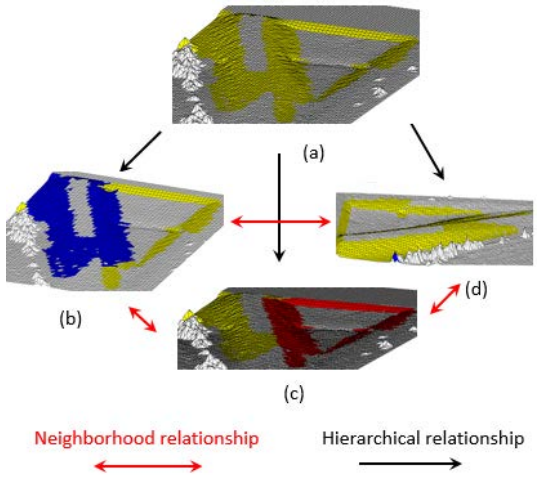

Figure 9 (a) Landform segmentation decompose to (b & d) two horizontal convex structure and (c) one concave structure.

Figure 10 shows a complex building decomposed (See figure 8) to its constituent sub-objects including five horizontal convex structures and one concave structure.

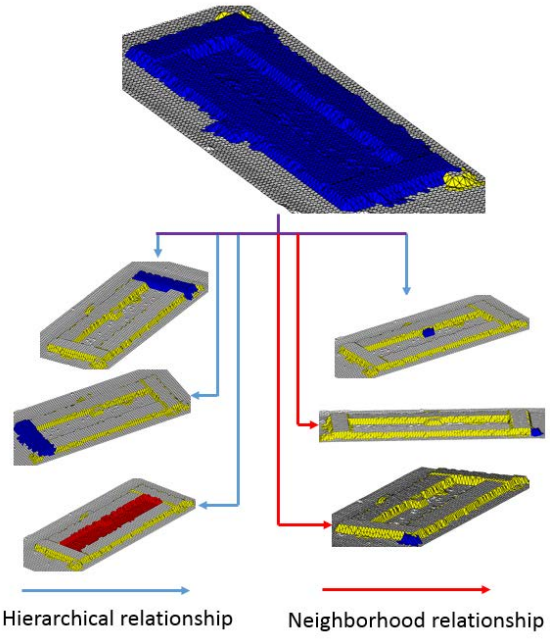

Figure 10 Complex building decompose to its constituent sub-objects.

Here in the figure, the hierarchical relationships among object and its sub-objects are only shown. It is to be noted

that there are two external objects at the side of the building that was included during the segmentation process, has also been extracted as external objects.

IV. Discussion

In this paper, we introduce a novel methodology for extracting object and its sub-objects - natural and man-made from LiDAR data. This virtual surveyor based object extraction technique can be integrated with an object-based classifier, which has proven to be more successful than the pixel-based classifier.

Due to the relative complexity of real-world objects and the difficulty in setting scale parameters tuned to each class of objects present in the scene, over-segmentation is an issue in the results of existing object extraction method. In our approach, the hierarchical decomposition can be conducted without traversing through multiple scales.

The future development plan will be to construct a fully automated virtual surveyor based object extraction algorithm where the seeds of all salient object of a given LiDAR data are automatically detected. The complete algorithm will be tested on a wide variety of terrain. Quantitative analysis will be performed to prove the efficacy of the algorithm.

V. Acknowledgements

This work was supported in part by a grant from the Natural Resources Conservation Service.

References

[1] S. Lang and T. Blaschke, “Hierarchical object representation-comparative multi-scale mapping of anthropogenic and natural features,” INTERNATIONAL ARCHIVES OF PHOTOGRAMMETRY REMOTE SENSING AND SPATIAL INFORMATION SCIENCES, vol. 34, no. 3/W8, pp. 181–186, 2003.

[2] T. Blaschke et al., “Geographic object-based image analysis–towards a new paradigm,” ISPRS Journal of Photogrammetry and Remote Sensing, vol. 87, pp. 180–191, 2014.

[3] H. Arefi and M. Hahn, “A hierarchical procedure for segmentation and classification of airborne LIDAR images,” in INTERNATIONAL GEOSCIENCE AND REMOTE SENSING SYMPOSIUM, 2005, vol. 7, p. 4950.

[4] Cheng and J. Han, “A survey on object detection in optical remote sensing images,” ISPRS Journal of Photogrammetry and Remote Sensing, vol. 117, pp. 11–28, 2016

[5] A. Golovinskiy, V. G. Kim, and T. Funkhouser, “Shape-based recognition of 3D point clouds in urban environments,” in 2009 IEEE 12th International Conference on Computer Vision, 2009, pp. 2154–2161.

[6] W. Yao, S. Hinz, and U. Stilla, “Object extraction based on 3D-segmentation of lidar data by combining mean shift with normalized cuts: Two examples from urban areas,” in 2009 Joint Urban Remote Sensing Event, 2009, pp. 1–6.

[7] R. A. MacMillan and P. A. Shary, “Landforms and landform elements in geomorphometry,” Developments in soil science, vol. 33, pp. 227–254, 2009.

[8] M. Baatz and A. Schäpe, “Multiresolution segmentation: an optimization approach for high quality multi-scale image segmentation,” Angewandte Geographische Informationsverarbeitung XII, vol. 58, pp. 12–23, 2000.

[9] L. Drăguț, O. Csillik, J. Minár, and I. S. Evans, “Land-surface segmentation to delineate elementary forms from Digital Elevation Models,” 2013.

[10] I. S. Evans, “Geomorphometry and landform mapping: What is a landform?,” Geomorphology, vol. 137, no. 1, pp. 94–106, 2012.

[11] M. F. Wu, Z. C. Sun, B. Yang, and S. S. Yu, “A Hierarchical Object-oriented Urban Land Cover Classification Using WorldView-2 Imagery and Airborne LiDAR data,” in IOP Conference Series: Earth and Environmental Science, 2016, vol. 46, p. 1, 2016.

[12] Blaschke, “Object based image analysis for remote sensing,” ISPRS journal of photogrammetry and remote sensing, vol. 65, no. 1, pp. 2–16, 2010.

[13] M. Musci, R. Q. Feitosa, and G. A. Costa, “An object-based image analysis approach based on independent segmentations,” in Urban Remote Sensing Event (JURSE), 2013 Joint, 2013, pp. 275–278.

[14] A. Habib and V. Devarajan, " Virtual Surveyor: an in-situ surveyor based segmentation to delineate landforms from airborne LiDAR returns," Imaging and Geospatial Technology Forum, IGTF 2016 - ASPRS Annual Conference and co-located JACIE Workshop. American Society for Photogrammetry and Remote Sensing, Fort Worth, Texas, 2016